International Journal of Modern Manufacturing Technologies
ISSN 2067–3604, Vol. XIV, No. 3 / 2022
https://doi.org/ 10.54684/ijmmt.2022.14.3.38

THREE-DIMENSIONAL MODELLING OF RAILS / WHEELS MANUFACTURED BY ER6 AND ER7 IN TRAMWAY APPLICATIONS

Elhocine Chiba, Mourad Abdelkrim, Abderrahim Belloufi, Imane Rezgui

Laboratory of Applied Mechanics and Energy Systems, Faculty of Applied Science, University of Kasdi Merbah, Ouargla 30000, Algeria

Corresponding author: Elhocine Chiba, chibaelhocine@gmail.com

Abstract: The wheels and rails of the train, tram etc. are often verified from their microstructure and plastic deformation, which usually appear in the outer layer of a wheel and rail, to analyse the causes of geometrical defects by monitoring the applied loads and variation of the temperature as suggested in the literature. This paper studies the effect of thermal stress applied with variations of the loads in contact on wheel/rail for the tramway, tracking through the state of the rail to discover the causes of geometric defects started by temperature variations and loads, and applying these variations of temperature and loads to know its resistance to these climatic conditions. 3D model of temperature distrubtion and heat flow in the wheel and the rail ER6 and ER7 has been developped using the finite element method based on the COMSOL Multiphisics.

Key words: *wheel*-rail, geometric defect, thermal stress, tramway, FEM.

1. INTRODUCTION

Linked to wheel/rail contact, they are often researched The study of rolling contact is of interest to both academia and industry, owing to the complexity inherent in dealing with the vast array of variables affecting the transfer of forces between the train and the track, as well as the wear rates of wheels and rails. The grade aimed for rail production is evaluated regarding welding ability. The steel joints were MAG welded and characterized regarding fatigue life. Railway rails are subjected to complex dynamic loading, which promotes the fatigue crack propagation phenomenon [1] As newer demands for faster and more heavily loaded trains emerge [2]. To ensure railway system security and reduce service costs, it is required to characterize the mechanical behavior of the zone containing metal ripping induced by a manufacturing flaw that may be the cause of breakage [3]. These connections that predict surface temperature evolution can be used as time-dependent boundary conditions, making sliding body thermal analysis independent [4].

Damages to the wheel are classified as tread contact fatigue, braking thermal fatigue, and web plate mechanical fatigue. The railway wheel's initial residual stress is produced during manufacturing and changes owing to thermal stress during braking [5]. M. Bin Sudin et al. [6] found that the interaction rail-wheel cause wear damage and friction-heat by predicting the contact temperature due to load and velocity. Using Adomian's decomposition technique, the temperature increase was calculated numerically. Peak pressure distributions rise linearly with applied load, with a slope of 0.053. Maximum temperature rise was 259.98 K at 1 mm, 5.3 MPa, and 3.14 m s^{-1}. Temperature changes in the wheel-rail contact zone and thermally affected sliding surfaces affect microstructural evolution in wear and fatigue.

Zhu, J. et al. [7] have shown how the traction coefficient affects the stresses in the wheel/rail contact zone. The theoretical thermal method for temperature variation and the finite element method to estimate contact thermal stresses improved knowledge of wheel/rail contact in various contact conditions (dry, wet and oily). Results show that environmental factors have no effect on normal contact zone stresses. Depending on frictional conditions, Von-Mises stress and lateral and longitudinal stress components can vary significantly. Environmental conditions also influenced the contact zone temperature rise.

Fatigue Crack Growth impacts structural integrity. Numerical approaches are required when complicated geometry or stress conditions cause mixed mode fatigue fracture propagation.

While both wear and fatigue are inextricably partly and are frequently considered mutually exclusive. The wear of railway wheels and rails is typically investigated by comparing the wear rate to the (T/A) parameters or by plotting so-called "wear maps" that show the relationship between various rolling parameters and the wear rate, [8]. The defects caused by thermal stress interacting with other loads include pinch points, rolling contact fatigue, and deformation.

In the presence of railway traction effects, there are different forces. Among these forces, it is the thermal forces linked to the conditions of traction control at the different zones of the stop [9].

When the wheel is running on rail, frictional energy is generated and converted into heat while a wheel is on rail.

When the wheel is running on rail, frictional energy is generated and converted into heat. To evaluate the contribution of thermal effects and plasticity, five different material models were studied among them TEPS by [10]. The camera flash temperature in a rail asperity caused by wheel-rail rolling contact, total heat produced, and high efficiency are also investigated. The distribution of contact intensity factor considers contact area roughness, friction, and plastic deformation [11].

The critical creepage rail temperature proved the martensitic heat transfer capability. Synchronization impact provides earlier damage at smaller creepage.

Suchánek, A., et al. [12] detected of reduced stress on a braked railway wheel, based on thermal transient analysis on virtual models, which influence the characteristics of the railway wheels. Structural analysis was performed by means of the ANSYS Multiphysics program system package. Thermal transient analysis deals with detection of temperature fields which are a result of braking by brake block, and the applied heat flux represents the heat generated by friction of brake block.

The pressure contact between wheel and rail under different contact conditions it's important. The dry, wet, and greasy environmental interactions were modelled with friction coefficients of 0.4, 0.2, and 0.07, [13]. The high mechanical stresses at the contact area raise the temperature, reducing the wheel/yield rail's strength. Temperature rise is a primary cause of microstructure changes on rail surfaces, specifically the creation of White Etching Layer. The model's results show that external factors have little effect on normal contact stress, pressure, and area. Depending on the friction conditions, the Von-Mises stress and lateral and longitudinal stress components might vary dramatically. The temperature rise at the contact zone is also influenced by the environment.

K. Knothe et al. [14] analyzed sliding component contact and temperature fields using laplacian transforms and Green's functions various pressure distributions on an elliptical contact area with surface abrasion and indentations are also possible. Calculations show pressure increases contact temperature by 30%. Wheel-rail systems can't exceed 500°C. Only modern wheel-slip regulated traction drives (creeps much above 1%) and high running speeds can reach 600°C for martensitic transformation. Thermally-induced surface tensions affect tribology.

The interaction between rail and wheel materials produces wear damage on each surface and frictional heat, [15]. Used frictional heat as a solid contact pressure to forecast contact temperature between rail and wheel for varied loads and speeds, as the applied load increases, the peak pressure distributions expand linearly with an average value of 0.053. Thermal expansion with x = 1mm and 3.14 m s^{-1} sliding speed was 259.98 K. The pin-on-disc approach was used to validate the temperature rise prediction. The average prediction error was 4.99 %.

Using finite element analysis, Seo, J.W., et al., [8] assessed residual stress of web plate owing to heat treatment and braking. The finite element approach is used to determine the cyclic stress history. The web plate's fatigue strength is tested to see how residual stress affects it.

The total emissivity of mild steel specimens at high temperatures was calculated numerically (Sadiq H., et al., [16]). In this procedure, a steel specimen and its surrounding heating environment are considered to be in thermal equilibrium. The numerical model's convective heat transfer coefficient was thoroughly investigated utilizing transient high temperature experiments. This study's steel emissivity data demonstrates that steel emissivity fluctuates with temperature, with a sharper variation between 400 and 500°C. Steel emissivity at high temperatures is recommended for steel design in fire.

The cyclic loading of railway wheel specimens was studied experimentally and numerically. The same condition of rigid-insert fracture closure model was used on a railway wheel specimen. The results show that specimen fatigue life reduces with increasing load level, [17].

The aim of this study is to focus on the importance of the chemical composition of the rail and wheel to resist different climatic conditions and to ensure good contact between the wheel and the rail for ease of movement of the rail vehicle in the Saharan area of the Ouargla tramway, depending on the loads applied and the change in the temperature of the rail. A finite element - based model has been developed to understand the different phenomena applied on the rail, using the COMSOL Multiphysics code.

2. DESCRIPTION AND SIMULATION

To understand the phenomenon of distribution the temperature of rail especially in the contact, particularly on railway bridges, a model based on finite elements has been developed with the COMSOL Multiphysics. The model considered in this study consists of a simple rigid wheel and rail.

This approach makes it possible to check the contact between two rigid bodies on the one hand, and the

contact between the rigid and flexible bodies on the other hand.

2.1.Description of ER6, ER 7 and ER8

The chemical composition of rail and wheel steel are described in table 1 so that the simulation of this distribution closer than reality.

2.2. Rail temperature measurement

Temperature and thermal forces play an important role and as the region is a desert and dry throughout the year, for this we choose measuring this temperature during the summer using the optical byromter; because it reaches 70 °C under the sun at noon as indicated in the figure 1.

Table 1. Chemical Composition of Steel ER6, ER7 and ER8 [18-19].

%	C	Si	Mn	P b	S	Cr	Cu	Mo	Ni	V
ER6	≤0.48	≤0.40	≤0.75	≤0.020	≤0.015	≤0.30	≤0.30	≤0.08	≤0.30	≤0.06
ER7	≤0.52	≤0.33	≤0.73	≤0.013	≤0.009	≤0.25	≤0.12	≤0.03	≤0.08	≤0.01
ER8	≤0.56	≤0.40	≤0.80	≤0.020	≤0.015	≤0.30	≤0.30	≤0.08	≤0.30	≤0.06

Table 2. The mechanical characteristics of steel ER6, ER7 and ER8 [18-19].

	ER7 and ER6	ER8
E (Young's modulus)	$2.1.10^5$ (MPa)	$2.1.10^5$ (MPa)
Poisson's ratio	0.3	0.3
Rm	678 (MPa)	860/980 (MPa)

Fig. 1. Optical byromter.

In addition, the conditions of the desert climate of the city of Ouargla have a significant impact on the rails especially during the summer period, this temperature reaches 70 °C during the day and drops to 40 °C at night.

The figure 2 shows the evolution of temperature of the rail at the afternoon according to the days during the month of July.

We see from the figure that the measured rail temperature remains constant in the value of 60 °C and does not change significantly until the days have passed.

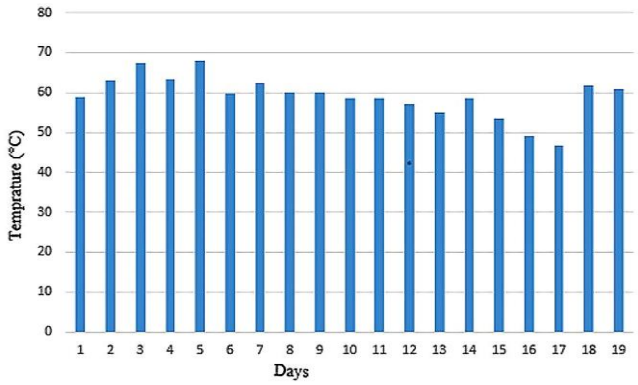

Fig. 2. Temperatures in the afternoon rail of month of July for year 2021.

2.3. Description the model of wheel and rail

A three-dimensional model is created using the COMSOL Multiphysics software, based on the actual geometrical properties Table 1 and Table 2 of the wheel/rail. The geometrical model of wheel/rail is meshed using the triangular elements figure 3, these elements are full integration elements and the choice of this type of element is based on the geometric configuration of the whole 3D model and also taking into account the heat diffusion.

In addition to this, the mesh is selected based on the shortest possible length of the rail or the wheel, with consideration given to the initial conditions as well as the physical parameters that will be used.

The resolution of the heat transfer problem of the wheel/rail, taking into the account all the boundary conditions is mad in stationary state from the discretization of the heat transfer equation integrated in the calculation code of software - equation (1) and equation (2).

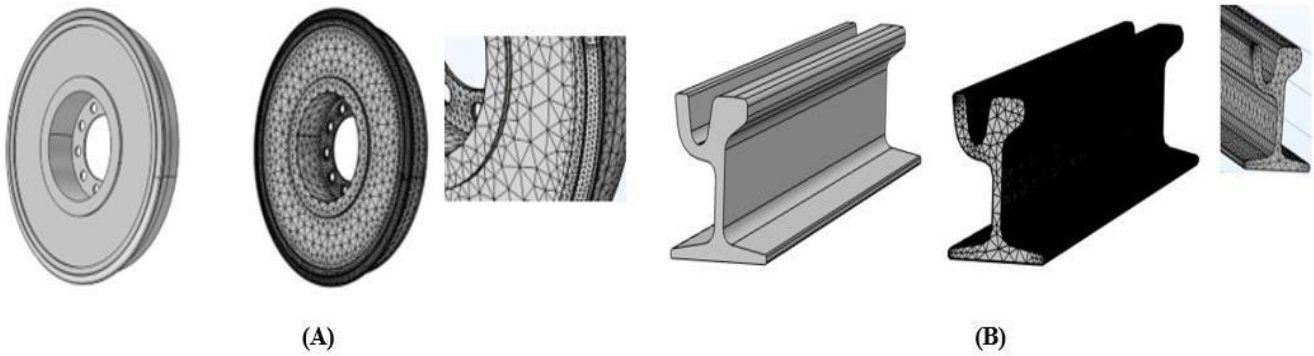

(A) (B)

Fig. 3. 3D finite element model of: (A) wheel, (B) rail

$$\rho C_p \mu.\nabla T + \nabla.q = Q + Q_{ted} \quad (1)$$

$$q = -K\nabla T \quad (2)$$

Where:

ρ: Densite (kg/m^3).

C_p: Heat capacity at constant pressure (J/kg. K).

μ: Fluid velocity vector (m/s).

T: Temperature (K).

Q: Heat source (W/m^3).

Q_{ted} : Thermoelastic damping (W/m^3).

q: Conductive heat flux (W/m^2).

K: Thermal conductivity (W/m.k).

3. RESULTS AND DISCUSSION

Among the obtained results, we depicted in figure 4 and figure 5 the temperature distribution with Von Mises pressure under Heat Transfer in Solids with:

The figure 4 demonstrates how the temperature rises as we approach the point of contact between the rail and wheel, where the wheel is directly subjected to frictioal force with different load applied.

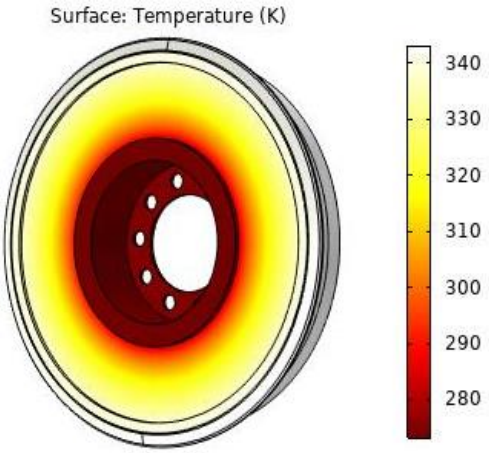

(A)

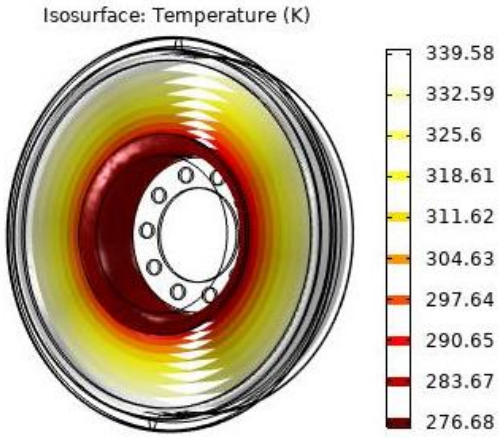

(B)

Fig. 4. Distribution of temperature on wheel (°K)

On the other hand, the figure 4 (A) and 4 (B) illustrates the evolution of thermal field and the isotherms in the wheel. The figure shows that the temperature clearly increases the closer we get to the point of the contact wheel/rail.

The figure 5 illustrates the evolution of thermal field and the isotherms in the rail. Also the figure shows that the temperature clearly increases the closer we get to the point of the contact rail/wheel, where the rail is exposed to the sun throughout the day.

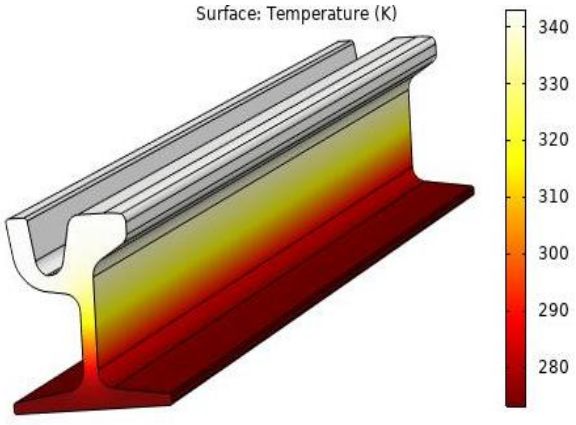

(A)

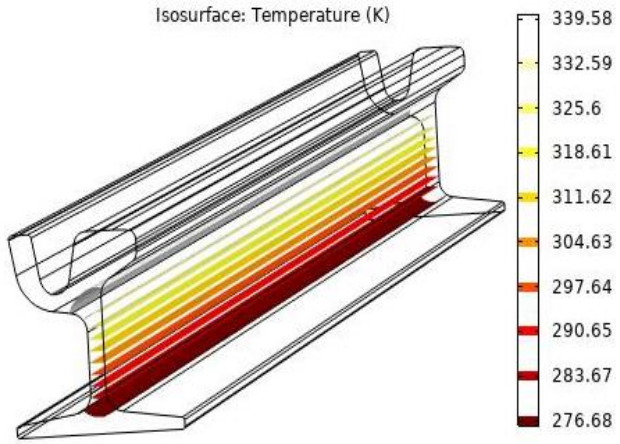

(B)

Fig. 5. Distribution of temperature on rail (°K)

Several types of heat exchangers, representing a range of sizes and flow configurations, are presented in the Application Library's Heat exchangers section integrated in COMSOL software.

Figure 5 (B) illustrates that the field distribution of the temperature of the head of the rail towards the rail pad is transmitted in the form of a field of temperature represented in the wall of the rail.

Figure 6 represents the evolution of the temperature in the rail as a function of the length of the rail.

Horizontal line illustrated in this figure indicated the temperature distribution. A stable temperature distribtion from 0 to 3m of the rail length was observed with a temperature range 322.59 K to 322.73 K.

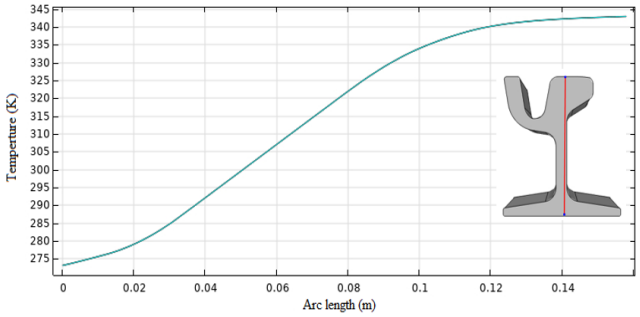

Fig. 7. Temperature distribution (K) by to the arc lengt vertical (m).

Variation of temperature is illustred in the figure 7. Temprture distribution is obtined in the cross section according to the red line. A decrease in temperature distribution from the head of rail to its bottom was observed. The maximum temperature is 345 K while the minimum value 275 K.

From those results, we can conclude the importance of monitoring the evolution of the temperature on the wheel/rail and its effect on the appearance of the corrugate wear and deformations.

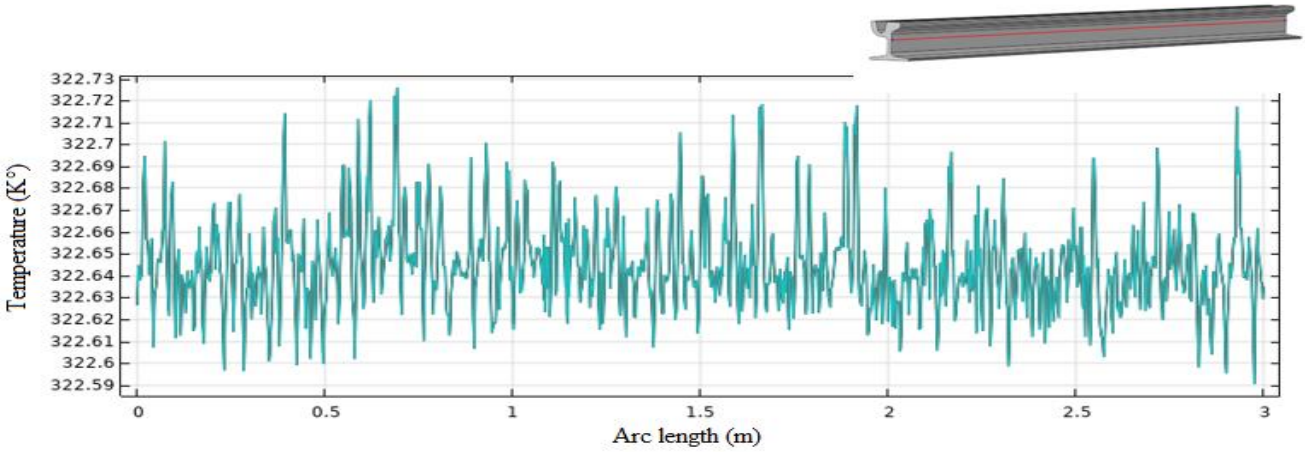

Fig. 6. Temperature distribution (K) by to the arc lengt horizontal (m).

4. CONCLUSIONS

In this work, a study of the distribution of temperatures on wheels and rails on the railways ER6 and ER7 in the Saharan area of the Ouargla tramway was presented.

The temperature distribution in the wheel and rail obtained by simulation with COMSOL Multiphysique. Taking into account all of the Sharan conditions, the maximum temperature recorded in the rail was reached 70°C under sun in the summer period.

Based on the numerical simulation by the finite element method using COMSOL Multiphysics, we concluded:

- The monitoring wheel/rail temperature in our sharian region is importante, especially during the summer period when the temperature measured under the sun is over 70 °C.
- Thermal stress in the metal of the rail or the wheel is resulted from a sudden decrease or increase in temperature, thus it negatively affects the lifespan of

the rail and wheel.
- The 3D model developped by COMSOL Multiphsic helped us to understand the distribution of heat flow in the wheel and rail.

5. REFERENCES

1. Baptista, R., et al., (2018). *Fatigue behavior and microstructural characterization of a high strength steel for welded railway rails,* International Journal of Fatigue, 117, 1-8.
2. Soares, H., et al., (2016). *Experimental characterization of the mechanical properties of railway wheels manufactured using class B material,* Procedia Structural Integrity, 1, 265-272.
3. Boussalia, L., Bellaouar, A., (2016). *Numerical study of the mechanical behaviour of railway wheels containing tearing on the tread,* Third International Conference on Energy, Materials, Applied Energetics and Pollution Constantine, Algeria, pp. 580-585.
4.Alizadeh Otorabad, H., et al., (2018). *Analytical formulation for temperature evolution in flat wheel-rail sliding surfaces,* Mathematical Problems in Engineering, 2018, 4239658.
5. Seo, J.W., et al., (2009). *Effects of residual stress and shape of web plate on the fatigue life of railway wheels,* Engineering Failure Analysis, 16(7), 2493-2507.
6.Sudin, M.B. and M. Baharom, (2012). *Prediction of contact temperature on interaction between rail and wheel materials using Pin-on-Disc method,* Journal of Applied Sciences, 12(23), 2424-2429.
7.Vo, K.D., et al., (2014). *A tool to estimate the wheel/rail contact and temperature rising under dry, wet and oily condition,* Computers in Railways XIV: Railway Engineering Design and Optimization, Brebbia, C.A., Tomii, N., Tzieropoulos, P., Mera, J.M. (eds.), 135, WIT Press, 191-201.
8. Vicente, F.S., Guillamón, M.P., (2019). *Use of the fatigue index to study rolling contact wear,* Wear, 436, 203036.
9.Wei, Y., Wu, Y., Duan, Z., (2014). *Thermal and dynamic behaviors of wheel/rail contact system considering thermal-mechanical coupling effects,* Journal of Vibroengineering, 20(6), 2414-2423.
10. Naeimi, M., et al., (2018). *Thermomechanical analysis of the wheel-rail contact using a coupled modelling procedure,* Tribology International, 117, 250-260.
11. Fischer, F., Daves, W., Werner, E., (2003). *On the temperature in the wheel–rail rolling contact,* Fatigue & Fracture of Engineering Materials & Structures, 26(10), 999-1006.
12. Suchánek, A., et al., (2018). *Analysis of the distribution of temperature fields in the braked railway wheel,* MATEC Web of conferences EDP Sciences, 157, 02048.
13.Knothe, K., Liebelt, S., (1995). *Determination of temperatures for sliding contact with applications for wheel-rail systems,* Wear, 189(1), 91-99.
14. Sudin, M.B., Baharom, M., (2012). *Prediction of contact temperature on interaction between rail and wheel materials using Pin-on-Disc method,* Journal of Applied Sciences, 12(23), 2424-2429.
15. Sadiq, H., et al., (2013). *Determination of steel emissivity for the temperature prediction of structural steel members in fire,* Journal of Materials in Civil Engineering, 25(2), 167-173.
16. Nejad, R.M., Berto, F., (2021). *Fatigue fracture and fatigue life assessment of railway wheel using non-linear model for fatigue crack growth,* International Journal of Fatigue, 153, 106516.
17. Vicente, F.S. and M.P. Guillamón, (2019). *Use of the fatigue index to study rolling contact wear.* Wear, 436, 203036.

Received: March 30, 2022 / Accepted: December 15, 2022 / Paper available online: December 20, 2022 © International Journal of Modern Manufacturing Technologies